

PHONON DISPERSION IN GRAPHENE

*L. A. Falkovsky**

*Landau Institute for Theoretical Physics, Russian Academy of Sciences
117334, Moscow, Russia*

*Institute of High Pressure Physics, Russian Academy of Sciences
142190, Troitsk, Moscow Region, Russia*

Received February 19, 2007

Taking the constraints imposed by the lattice symmetry into account, we calculate the phonon dispersion for graphene with interactions between the first and second nearest neighbors. We show that only five force constants give a very good fitting to the elastic constants and phonon frequencies observed in graphite.

PACS: 63.20.Dj, 81.05.Uw, 71.15.Mb

1. INTRODUCTION

Since the discovery of graphene (a single atomic layer of graphite) [1, 2], much attention has been devoted to its electronic properties. Now, Raman spectroscopy [3] extends to investigations of graphene. For interpretations of the Raman scattering and of the transport phenomena, the detailed knowledge of the lattice dynamics and the electron–phonon interactions is needed [4].

Several models [5–12] have been proposed to calculate the phonon dispersion in bulk graphite. Most improved ones [9, 10] involve many (up to twenty) parameters. Recently, the detailed measurements and first-principle calculations of optical phonon frequencies were made for graphite [13]. They show the qualitative disagreement with the models [5, 12], employing the central and angular atomic forces between the first and second neighbors in the graphite lattice.

The passage in the lattice dynamics from graphite to graphene and then to nanotubes was examined in Ref. [14] using the model in [5]. Numerical calculations of the dynamical matrix in terms of the electron energy for graphene were performed in [15]. The first-principle calculations [16] of the dynamical properties of graphite and graphene (and also of diamond) show that differences between the phonon frequencies in graphene and the related ones in graphite are negligible in comparison with the experimental errors for these frequencies in graphite. This could be intuitively expected for the

highest frequencies because interactions between the layers in graphite are weak.

Our aim here is to find an analytic description of the phonon dispersion in graphene. This can be done in the framework of the Born–von Karman model for the honeycomb graphene lattice with interactions only between the first and second nearest neighbors, but with the constraints imposed by the lattice symmetry taken into account. We find that the out-plane (bending) modes are described by two force constants, one of which is determined by the corresponding Raman frequency and the other by the smallest elastic constant C_{44} . For the in-plane modes, the lattice stability condition with respect to rotation of the layer as a whole around the z axis allows reducing the number of force constants to three. These constants are extracted from comparison with experimental data for graphite. We do not pay close attention to the agreement of lower frequencies with experiment because their values in graphene are convincingly smaller than the ones in graphite. The extent of agreement of the present theory with experiments corresponds to the comparison level between the first-principle calculations by the authors of Ref. [13] and their experimental data (see Table 2 below).

2. PHONON DYNAMICS IN THE NEAREST-NEIGHBOR APPROXIMATION

The equations of motion in the harmonic approximation are written in the well-known form

*E-mail: falk@itp.ac.ru

$$\sum_{j,m,\kappa'} \Phi_{ij}^{\kappa\kappa'}(\mathbf{a}_n - \mathbf{a}_m) u_j^{\kappa'}(\mathbf{a}_m) - \omega^2 u_i^\kappa(\mathbf{a}_n) = 0, \quad (1)$$

where the vectors \mathbf{a}_n label lattice cells, the superscripts “ κ ” and “ κ' ” denote two sublattices A and B , and the subscripts $i, j = x, y, z$ take three values corresponding to the spatial coordinates. Since the potential energy is a quadratic function of the atomic displacements $u_i^A(\mathbf{a}_n)$ and $u_i^B(\mathbf{a}_n)$, the dynamical matrix can be taken in the symmetric form:

$$\Phi_{ij}^{AB}(\mathbf{a}_n) = \Phi_{ji}^{BA}(-\mathbf{a}_n).$$

Its Fourier transform is then a Hermitian matrix. Each atom, for instance \mathbf{A}_0 (Fig. 1), has three first neighbors in the other sublattice, i.e., B , with the relative vectors

$$\mathbf{B}_1 = a(1, 0), \quad \mathbf{B}_{2,3} = a(-1, \pm\sqrt{3})/2$$

and six second neighbors in the same sublattice A with the relative vectors

$$\mathbf{A}_{1,4} = \pm a(0, \sqrt{3}), \quad \mathbf{A}_{2,5} = \pm a(-3, \sqrt{3})/2,$$

$$\mathbf{A}_{3,6} = \mp a(3, \sqrt{3})/2,$$

where $a = 1.42 \text{ \AA}$ is the carbon-carbon distance.

For the nearest neighbors (in the B sublattice), the Fourier transform of the dynamical matrix is given by

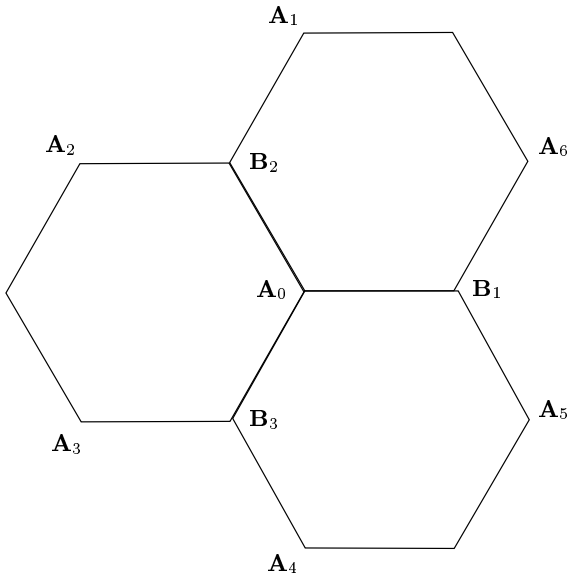


Fig. 1. First and second neighbors in the graphene lattice

$$\begin{aligned} \phi_{ij}^{AB}(\mathbf{q}) &= \sum_{\kappa=1}^3 \Phi_{ij}^{AB}(\mathbf{B}_\kappa) \exp(i\mathbf{q}\mathbf{B}_\kappa) = \\ &= \Phi_{ij}^{AB}(\mathbf{B}_1) \exp(iq_x) + \Phi_{ij}^{AB}(\mathbf{B}_2) \times \\ &\quad \times \exp\left[i\left(-q_x + q_y\sqrt{3}/2\right)\right] + \\ &\quad + \Phi_{ij}^{AB}(\mathbf{B}_3) \exp\left[i\left(-q_x - q_y\sqrt{3}/2\right)\right], \quad (2) \end{aligned}$$

where the wave vector \mathbf{q} is taken in units of $1/a$. For the next neighbors (in the A sublattice), we write

$$\phi_{ij}^{AA}(\mathbf{q}) = \Phi_{ij}^{AA}(\mathbf{A}_0) + \sum_{\kappa=1}^6 \Phi_{ij}^{AA}(\mathbf{A}_\kappa) \exp(i\mathbf{q}\mathbf{A}_\kappa), \quad (3)$$

where \mathbf{A}_0 labels the atom chosen at the center of the coordinate system in the A sublattice.

Symmetry considerations impose constraints on the dynamical matrix. To obtain them, we introduce variables $\xi, \eta = x \pm iy$ transforming under the C_3 rotation around the z axis (taken at the \mathbf{A}_0 atom) as

$$(\xi, \eta) \rightarrow (\xi, \eta) \exp(\pm 2\pi i/3).$$

Under the rotation, the atoms change their positions as

$$\mathbf{B}_1 \rightarrow \mathbf{B}_2 \rightarrow \mathbf{B}_3, \quad \mathbf{A}_1 \rightarrow \mathbf{A}_3 \rightarrow \mathbf{A}_5,$$

$$\mathbf{A}_2 \rightarrow \mathbf{A}_4 \rightarrow \mathbf{A}_6.$$

Therefore, all the force constants $\Phi_{\xi\eta}^{AB}(\mathbf{B}_\kappa)$ with the different κ (as well as $\Phi_{zz}^{AB}(\mathbf{B}_\kappa)$) are equal to one another. Moreover, these constants are real because the reflection $x \rightarrow x, y \rightarrow -y$ belongs to the symmetry group of the sublattices.

We similarly find

$$\begin{aligned} \Phi_{\xi\xi}^{AB}(\mathbf{B}_1) &= \Phi_{\xi\xi}^{AB}(\mathbf{B}_2) \exp(2\pi i/3) = \\ &= \Phi_{\xi\xi}^{AB}(\mathbf{B}_3) \exp(-2\pi i/3), \quad (4) \end{aligned}$$

because they transform as covariant variables. The relation between $\Phi_{\xi\xi}^{AA}(\mathbf{A}_\kappa)$ for $\kappa = 1, 3, 5$ (and also for $\kappa = 2, 4, 6$) has the same form. For the atom \mathbf{A}_0 , there are two real force constants, $\Phi_{\xi\eta}^{AA}(\mathbf{A}_0)$ and $\Phi_{zz}^{AA}(\mathbf{A}_0)$.

2.1. Dispersion of the out-plane modes

In the first- and second-neighbor approximation, the out-plane vibrations u_z^A and u_z^B in the z direction are not coupled to the in-plane modes. The corresponding matrix for the out-plane modes has the form

$$\begin{pmatrix} \phi_{zz}^{AA}(\mathbf{q}) & \phi_{zz}^{AB}(\mathbf{q}) \\ \phi_{zz}^{AB}(\mathbf{q})^* & \phi_{zz}^{AA}(\mathbf{q}) \end{pmatrix}, \quad (5)$$

where

$$\phi_{zz}^{AA}(\mathbf{q}) = \Phi_{zz}^{AA}(\mathbf{A}_0) + 2\Phi_{zz}^{AA}(\mathbf{A}_1) \times \left[\cos(\sqrt{3}q_y) + 2 \cos\left(\frac{3q_x}{2}\right) \cos\left(\frac{\sqrt{3}q_y}{2}\right) \right],$$

$$\phi_{zz}^{AB}(\mathbf{q}) = \Phi_{zz}^{AB}(\mathbf{B}_1) \times \left[\exp(iq_x) + 2 \exp\left(-\frac{iq_x}{2}\right) \cos\left(\frac{\sqrt{3}q_y}{2}\right) \right].$$

The invariance with respect to the translation of the layer as a whole in the z -direction imposes the condition

$$\Phi_{zz}^{AA}(\mathbf{A}_0) + 6\Phi_{zz}^{AA}(\mathbf{A}_1) + 3\Phi_{zz}^{AB}(\mathbf{B}_1) = 0. \quad (6)$$

The phonon dispersion for the out-plane optical and acoustic modes is found as

$$\omega_{ZO,ZA}(\mathbf{q}) = \sqrt{u \pm v}, \quad (7)$$

where we introduce the notation

$$u = 2\gamma_z \left[\cos(\sqrt{3}q_y) + 2 \cos\left(\frac{3q_x}{2}\right) \cos\left(\frac{\sqrt{3}q_y}{2}\right) - 3 \right] - 3\alpha_z,$$

$$v = \alpha_z \left[1 + 4 \cos^2\left(\frac{\sqrt{3}q_y}{2}\right) + 4 \cos\left(\frac{3q_x}{2}\right) \cos\left(\frac{\sqrt{3}q_y}{2}\right) \right]^{1/2}.$$

The force constants $\alpha_z = \Phi_{zz}^{AB}(\mathbf{B}_1)$ and $\gamma_z = \Phi_{zz}^{AA}(\mathbf{A}_1)$ are real.

The last equations allow us to express the phonon frequencies of the out-plane branches at the critical points Γ , K , and M in terms of the force constants:

$$\omega_{ZO}(\Gamma) = \sqrt{-6\alpha_z}, \quad \omega_{ZO}(K) = \sqrt{-3\alpha_z - 9\gamma_z}, \quad (8)$$

$$\omega_{ZO}(M) = \sqrt{(-3 \mp 1)\alpha_z - 8\gamma_z}.$$

Expanding Eq. (7) in powers of the wave vector \mathbf{q} , we find the velocity of the acoustic out-plane mode propagating in the layer,

$$s_z = a \sqrt{-\frac{3}{4}\alpha_z - \frac{9}{2}\gamma_z} = \sqrt{\frac{C_{44}}{\rho}}, \quad (9)$$

where we use the well-known formula for the velocity of the acoustic z -mode propagating in the x direction in terms of the elastic constant C_{44} and density ρ of a hexagonal crystal. Because the interaction between the layers in graphite is weak, we can attribute values of C_{44} and ρ to graphite.

2.2. Force constants and frequencies of in-plane modes

The dynamical matrix for the in-plane vibrations has the form

$$\begin{pmatrix} \phi^{AA}(\mathbf{q}) & \phi^{AB}(\mathbf{q}) \\ \phi^{BA}(\mathbf{q}) & \phi^{BB}(\mathbf{q}) \end{pmatrix}, \quad (10)$$

where the 2×2 matrices $\phi(\mathbf{q})$ are

$$\phi^{AA}(\mathbf{q}) = \begin{pmatrix} \phi_{\xi\eta}^{AA}(\mathbf{q}) & \phi_{\xi\xi}^{AA}(\mathbf{q}) \\ \phi_{\xi\xi}^{AA}(\mathbf{q})^* & \phi_{\xi\eta}^{AA}(\mathbf{q}) \end{pmatrix} \quad (11)$$

with

$$\phi_{\xi\eta}^{AA}(\mathbf{q}) = 2\gamma \left[\cos(\sqrt{3}q_y) + 2 \cos\left(\frac{3q_x}{2}\right) \cos\left(\frac{\sqrt{3}q_y}{2}\right) - 3 \right] - 3\alpha,$$

$$\phi_{\xi\xi}^{AA}(\mathbf{q}) = \delta \left[\exp(i\sqrt{3}q_y) + 2 \cos\left(\frac{3q_x}{2} + \frac{2\pi}{3}\right) \times \exp\left(-\frac{i\sqrt{3}q_y}{2}\right) \right] + \delta^* \left[\exp(-i\sqrt{3}q_y) + 2 \cos\left(\frac{3q_x}{2} - \frac{2\pi}{3}\right) \exp\left(\frac{i\sqrt{3}q_y}{2}\right) \right],$$

and

$$\phi^{AB}(\mathbf{q}) = \begin{pmatrix} \phi_{\xi\eta}^{AB}(\mathbf{q}) & \phi_{\xi\xi}^{AB}(\mathbf{q}) \\ \phi_{\eta\eta}^{AB}(\mathbf{q}) & \phi_{\xi\eta}^{AB}(\mathbf{q}) \end{pmatrix} \quad (12)$$

with

$$\phi_{\xi\eta}^{AB}(\mathbf{q}) = \alpha \left[\exp(iq_x) + 2 \exp\left(-\frac{iq_x}{2}\right) \cos\left(\frac{\sqrt{3}q_y}{2}\right) \right],$$

$$\phi_{\xi\xi}^{AB}(\mathbf{q}) = \beta \left[\exp(iq_x) + 2 \exp\left(-\frac{iq_x}{2}\right) \cos\left(\frac{\sqrt{3}q_y}{2} - \frac{2\pi}{3}\right) \right],$$

$$\begin{aligned} \phi_{\eta\eta}^{AB}(\mathbf{q}) &= \\ &= \beta^* \left[\exp(iq_x) + 2 \exp\left(-\frac{iq_x}{2}\right) \cos\left(\frac{\sqrt{3}q_y}{2} + \frac{2\pi}{3}\right) \right], \end{aligned}$$

where

$$\begin{aligned} \alpha &= \Phi_{\xi\eta}^{AB}(\mathbf{B}_1), & \beta &= \Phi_{\xi\xi}^{AB}(\mathbf{B}_1), \\ \gamma &= \Phi_{\xi\eta}^{AA}(\mathbf{A}_1), & \delta &= \Phi_{\xi\xi}^{AA}(\mathbf{A}_1). \end{aligned}$$

The translation invariance condition similar to Eq. (6) was imposed on the force constants. The constants α and γ are evidently real. The constant β is real because the reflection $(x, y) \rightarrow (x, -y)$ with $B_1 \rightarrow B_1$ belongs to the symmetry group; the only one constant δ is complex.

The sublattice B can be obtained from A by the C_2 rotation $(x, y) \rightarrow -(x, y)$ of the graphene symmetry group. Therefore,

$$\begin{aligned} \phi_{\xi\xi}^{BB}(\mathbf{q}) &= \delta \left[\exp\left(-i\sqrt{3}q_y\right) + \right. \\ &+ 2 \cos\left(\frac{3q_x}{2} - \frac{2\pi}{3}\right) \exp\left(\frac{i\sqrt{3}q_y}{2}\right) \left. \right] + \\ &+ \delta^* \left[\exp\left(i\sqrt{3}q_y\right) + 2 \cos\left(\frac{3q_x}{2} + \frac{2\pi}{3}\right) \times \right. \\ &\quad \left. \times \exp\left(-\frac{i\sqrt{3}q_y}{2}\right) \right]. \quad (13) \end{aligned}$$

The optical phonon frequencies for the in-plane branches at Γ and K are found

$$\begin{aligned} \omega_{1,2}^{in-pl}(\Gamma) &= \sqrt{-6\alpha}, & \text{doublet}, \\ \omega_{1,2}^{in-pl}(K) &= \sqrt{-3\alpha - 9\gamma}, & \text{doublet}, \\ \omega_{3,4}^{in-pl}(K) &= \sqrt{-3\alpha - 9\gamma \pm 3|\beta|}. \end{aligned} \quad (14)$$

Using Eqs. (10)–(13), we can find the dispersion of in-plane modes for the G – K direction in the explicit form, but a fourth-order algebraic equation has to be solved for the M point as well as for points of the general position.

2.3. Elastic constants for in-plane modes

2.3.1. Condition following from the rotational symmetry

We already applied the conditions imposed on the force constants by the invariance under translations of the layer as a whole. The constants α , β , γ , and δ satisfy another condition resulting from the invariance under rotations of the layer around the z axis. Any atom

at the point $\mathbf{R}^\kappa(n)$ (in the lattice cell \mathbf{a}_n) is displaced under rotation by the vector with coordinates

$$u_x^\kappa(n) = \Omega R_y^\kappa(n), \quad u_y^\kappa(n) = -\Omega R_x^\kappa(n), \quad (15)$$

where Ω is the infinitesimal angle of the rotation, e.g., around the atom \mathbf{A}_0 . For the lattice stability, the force moment acting on the atom \mathbf{A}_0 from other atoms,

$$\sum_{n\kappa j} R_x^\kappa(n) \Phi_{yj}^{\kappa'\kappa}(n) u_j^\kappa(n) - R_y^\kappa(n) \Phi_{xj}^{\kappa'\kappa}(n) u_j^\kappa(n),$$

has to vanish for any Ω , i.e.,

$$\begin{aligned} \sum_{n\kappa} 2\Phi_{xy}^{\kappa'\kappa}(n) R_x^\kappa(n) R_y^\kappa(n) - \Phi_{xx}^{\kappa'\kappa}(n) R_y^\kappa(n)^2 - \\ - \Phi_{yy}^{\kappa'\kappa}(n) R_x^\kappa(n)^2 = 0. \end{aligned}$$

In terms of the ξ, η variables, we have

$$\begin{aligned} \Phi_{\xi\xi}^{\kappa'\kappa}(n) &= \Phi_{xx}^{\kappa'\kappa}(n) - \Phi_{yy}^{\kappa'\kappa}(n) - 2i\Phi_{xy}^{\kappa'\kappa}(n), \\ \Phi_{\xi\eta}^{\kappa'\kappa}(n) &= \Phi_{xx}^{\kappa'\kappa}(n) + \Phi_{yy}^{\kappa'\kappa}(n). \end{aligned} \quad (16)$$

Using these equalities, we obtain the lattice stability condition as

$$\begin{aligned} \sum_{n\kappa} 2\Phi_{\xi\eta}^{\kappa'\kappa}(n) R_\xi^\kappa(n) R_\eta^\kappa(n) - \Phi_{\xi\xi}^{\kappa'\kappa}(n) R_\eta^\kappa(n)^2 - \\ - \Phi_{\eta\eta}^{\kappa'\kappa}(n) R_\xi^\kappa(n)^2 = 0. \end{aligned}$$

Here, the term corresponding to the nearest neighbor \mathbf{B}_1 equals $2a^2[\alpha - \beta]$ and each other atom $\mathbf{B}_{2,3}$ gives the same contribution in accordance with Eqs. (4). From the next neighbor \mathbf{A}_1 , we obtain $6a^2[\gamma - \text{Re}\delta]$. Thus, summing up the contributions of the first and second neighbors, we find the rotational symmetry condition

$$\alpha - \beta + 6\gamma - 6\text{Re}\delta = 0. \quad (17)$$

2.3.2. Contribution of in-plane modes to the elastic constants

The in-plane vibrations make a contribution to the elastic constants C_{11} and C_{12} . The corresponding relation between the dynamical matrix elements and the elastic constants can be deduced by taking the long-wavelength limit ($\mathbf{q} \rightarrow 0$) in Eqs. (1), which we rewrite for the two-dimensional variables \mathbf{u}^A and \mathbf{u}^B as

$$\begin{aligned} (\phi^{AA} - \omega^2) \mathbf{u}^A + \phi^{AB} \mathbf{u}^B &= 0, \\ \phi^{BA} \mathbf{u}^A + (\phi^{BB} - \omega^2) \mathbf{u}^B &= 0 \end{aligned}$$

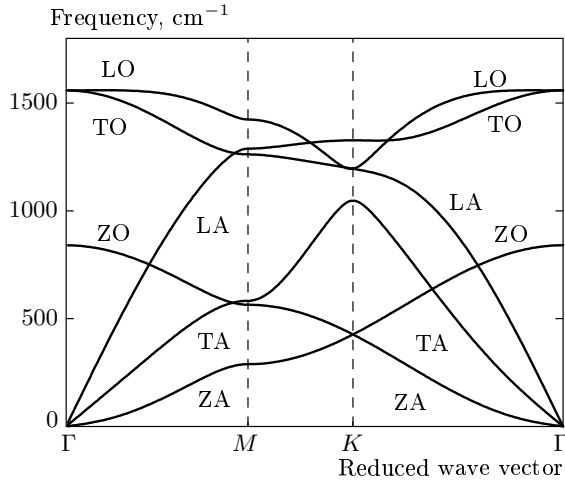


Fig. 2. Calculated phonon dispersion for graphene; Raman frequencies are listed in Table 1, the force constants and elastic constants are in Table 2

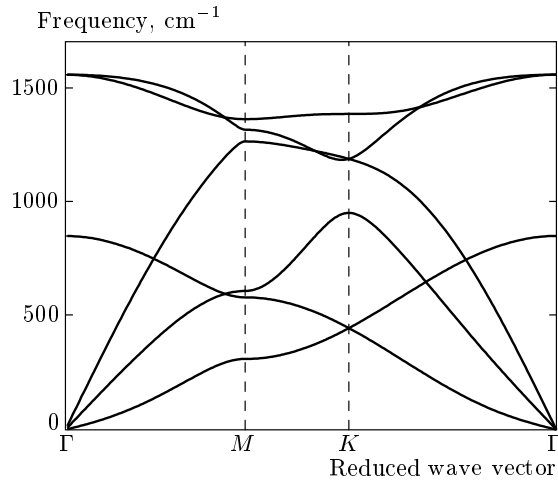


Fig. 3. A version of the phonon dispersion for graphene

using the form of matrix (10). Making the transformation

$$\mathbf{u}^A = \mathbf{u}^{ac} + \mathbf{u}^{opt}, \quad \mathbf{u}^B = \mathbf{u}^{ac} - \mathbf{u}^{opt}$$

to the new variables \mathbf{u}^{ac} and \mathbf{u}^{opt} , we obtain

$$\begin{aligned} (\phi^{AA} + \phi^{AB} - \omega^2) \mathbf{u}^{ac} + (\phi^{AA} - \omega^2 - \phi^{AB}) \mathbf{u}^{opt} &= 0, \\ (\phi^{BB} - \omega^2 - \phi^{BA}) \mathbf{u}^{opt} - (\phi^{BB} + \phi^{BA} - \omega^2) \mathbf{u}^{ac} &= 0. \end{aligned} \quad (18)$$

Expanding the matrices

$$\phi = \phi_0 + \phi_1 + \phi_2$$

in a series with respect to q , where the subscripts “0”, “1”, and “2” indicate the order of terms, we see that

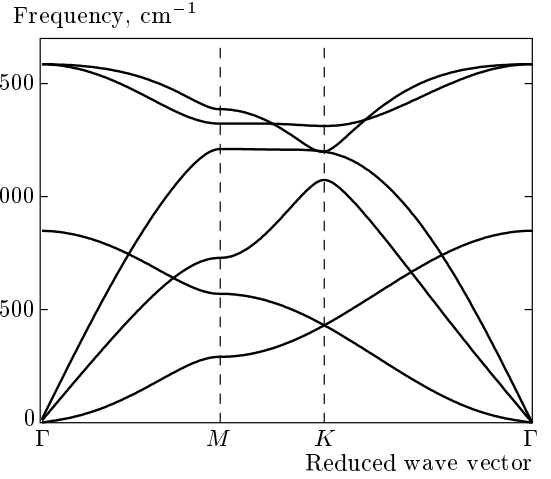


Fig. 4. Another version of the phonon dispersion for graphene

the diagonal terms in Eqs. (18) are of the first order because

$$\phi_0^{AA} + \phi_0^{AB} = 0$$

and $\omega \approx q$ for the acoustic modes. We can then eliminate $\mathbf{u}^{opt} \approx q$ from Eqs. (18). Using the notation

$$\phi_0 \equiv \phi_0^{AA} = \phi_0^{BB} = -\phi_0^{AB} = -\phi_0^{BA}$$

and calculating the inverse matrix, we find, to the first order,

$$(\phi_0 - \phi^{AB}/2)^{-1} = (1 + \phi_0^{-1} \phi_1^{AB}/2) \phi_0^{-1}.$$

For the acoustic modes \mathbf{u}^{ac} , we obtain

$$\begin{aligned} [(\phi^{AA} + \phi^{AB} + \phi^{BB} + \phi^{BA})/2 + \\ + \phi_1^{AB} \phi_0^{-1} \phi_1^{AB} - \omega^2] \mathbf{u}^{ac} = 0, \end{aligned} \quad (19)$$

where the subscripts “0” and “1” mean that terms of the zeroth and first order have to be kept, correspondingly, but the other expressions have to be expanded to the second order in \mathbf{q} . We find the matrix factor of \mathbf{u}^{ac} in Eqs. (19):

$$\begin{pmatrix} s_1 q^2 & s_2 q_+^2 \\ s_2^* q_-^2 & s_1 q^2 \end{pmatrix},$$

where

$$s_1 = -\frac{9}{2}\gamma - \frac{3}{4} \left(\alpha - \frac{\beta^2}{\alpha} \right), \quad s_2 = \frac{9}{4} \text{Re } \delta - \frac{3}{8}\beta.$$

We thus obtain the velocities of longitudinal and transverse acoustic in-plane modes related to the elastic constants

$$\frac{C_{11}}{\rho} = a^2(s_1 + |s_2|), \quad \frac{C_{11} - C_{12}}{2\rho} = a^2(s_1 - |s_2|). \quad (20)$$

Table 1. Lattice mode frequencies at critical points, in cm^{-1} (the superscripts “ z ” and “ \parallel ” stand for the out-plane and in-plane branches, correspondingly)

	Γ [00]		M [$1\sqrt{3}$] $\pi/3a$						K [01] $4\pi/s\sqrt{3}a$			
	ω^\parallel	ω^z	ω_1^\parallel	ω_2^\parallel	ω_3^\parallel	ω_4^\parallel	ω_1^z	ω_2^z	ω_1^\parallel	$\omega_{2,3}^\parallel$	ω_4^\parallel	$\omega_{1,2}^z$
Exp.	1590 ^a	861 ^a	1389 ^a			630 ^d	670 ^a	471 ^c	1313 ^d	1184 ^b		482 ^d
	1583 ^b	868 ^c	1390 ^b	1323 ^b	1290 ^b			451 ^d	1265 ^b	1194 ^b		517 ^d
	1565 ^b											
Theor. ^b	1581		1425	1350	1315				1300	1220	950	
Theor.	1558	840	1423	1288	1261	583	564	288	1326	1195	1047	426

^aReference [17], ^bReference [13], ^cReference [6], ^dReference [18].

Table 2. Force constants in 10^5 cm^{-2} and elastic constants (in 10 GPa), calculated (Theor.) and observed [19] (Exp.); the parameter $\gamma = -0.238 \cdot 10^5$ is determined from Eq. (17)

	α	β	δ	α_z	γ_z	C_{11}	C_{12}	C_{44}
Theor.	-4.046	1.107	-1.096	-1.176	0.190	92	24	0.43
Exp.						106 ± 2	18 ± 2	0.45 ± 0.05

3. FITTING WITH RAMAN AND ELASTIC DATA

The calculated phonon dispersion is shown in Fig. 2. We note, first, that the sound velocities (for the long waves, $q \rightarrow \Gamma$) have no dispersion in the xy plane, as it should be due to the C_6 symmetry of graphene. Second, the in-plane LO/TO modes at Γ , the in-plane LO/LA modes at K , and the out-plane ZA/ZO modes at K are doubly degenerate, because graphene is a nonpolar crystal and the symmetry of these points in the Brillouin zone includes the C_{3v} group with the two-dimensional representation (observation of splitting of those modes in graphene would display the symmetry breaking of the crystal).

Because of the lack of information about graphene, we compare the present theory with experiments on graphite. We prefer to obtain more accurate fitting for the higher frequencies because the absence of the neighboring layers in graphene affects low frequencies more intensely. Moreover, the low frequencies in graphene for the out-plane branches have to be less than their values in graphite, since the atoms are freer to move in the z direction in graphene than in graphite.

Thus, we have only two constants, α_z and γ_z , to fit four Raman frequencies of the out-plane modes and one elastic constant C_{44} (see Tables 1 and 2). The con-

stant α_z is determined by the Raman frequency ω_{ZO} , Eq. (8). The sound velocity s_z in Eq. (9) is very sensitive to small variations of γ_z and becomes complex for $\gamma_z > 0.2 \cdot 10^5 \text{ cm}^{-2}$. This indicates that graphene is nearly unstable with respect to transformation into a phase of the lower symmetry group at Γ . From the results of fitting, we can also see that the phonon frequencies for the z -modes are smaller than their values in graphite.

Fitting of the in-plane branches is insensitive to the imaginary part of the constant δ . Therefore, δ is taken as a real parameter. Thus, for the in-plane mode, we have to fit eight Raman frequencies and two elastic constants using three force constants. The fitting results are presented in Fig. 2 and in Tables 1 and 2. We note that the extent of agreement of the present theory with the data obtained for graphite corresponds to the comparison level between the first-principle calculations obtained by the authors of Ref. [13] for graphite and their experimental data (see Table 1). We see only qualitative discrepancy in the sequence of levels at M : in Fig. 2, the highest level is the LO mode, whereas the experiment appears to reveal a crossover of the TO and LO modes on the Γ - M line (similar to Γ - K line), yielding the TO mode higher at M . We examined the versions with the crossover, shown in Figs. 3 and 4.

The agreement with experiments is not so good in these cases as in the case shown in Fig. 2 and Tables 1 and 2, but the discrepancies of the order of 50 cm^{-1} between the different experiments, as well as the distinctions between graphene and graphite, do not allow choosing the version conclusively. The experiment on graphene would clarify this point.

4. CONCLUSIONS

We have calculated the phonon dispersion in graphene using the Born–von Karman model with only the first and second-neighbor interactions imposed by the symmetry constraints. The bending (out-plane) modes are not coupled to the in-plane branches and indicate the instability of graphene with respect to transformation into a lower-symmetry phase. The Raman frequencies of these modes are less than the corresponding values in graphite. The fitting of the higher in-plane modes shows good agreement of the calculated optical frequencies as well as of elastic constants with experiments.

The work was supported by the RFBR (grant No. 07-02-00571).

REFERENCES

1. K. S. Novoselov, A. K. Geim, S. V. Morozov et al., *Science* **306**, 666 (2004); *Nature* **438**, 197 (2005).
2. Y. Zhang, J. P. Small, M. E. S. Amory, and P. Kim, *Phys. Rev. Lett.* **94**, 176803 (2005).
3. C. C. Ferrari, J. C. Meyer, V. Scardaci et al., *Phys. Rev. Lett.* **97**, 187401 (2006).
4. A. H. Castro Neto and F. Guinea, *Phys. Rev. B* **75**, 045404 (2007).
5. J. De Launay, *Sol. St. Phys.* **3**, 203 (1957).
6. R. Nicklow, W. Wakabayashi, and H. G. Smith, *Phys. Rev. B* **5**, 4951 (1972).
7. A. A. Ahmadiéh and H. A. Rafizadeh, *Phys. Rev. B* **7**, 4527 (1973).
8. A. P. P. Nicholson and D. J. Bacon, *J. Phys. C* **10**, 2295 (1977).
9. M. Maeda, Y. Kuramoto, and C. Horie, *J. Phys. Soc. Jpn. Lett.* **47**, 337 (1979).
10. R. Al-Jishi and G. Dresselhaus, *Phys. Rev. B* **26**, 4514 (1982).
11. H. Gupta, J. Malhotra, N. Rani, and B. Tripathi, *Phys. Rev. B* **33**, 7285 (1986).
12. L. Lang, S. Doyen-Lang, A. Charlier, and M. F. Charlier, *Phys. Rev. B* **49**, 5672 (1994).
13. J. Maultzsch, S. Reich, C. Thomsen, H. Reequardt, and P. Ordejon, *Phys. Rev. Lett.* **92**, 075501 (2004).
14. A. Charlier, E. McRae, M.-F. Charlier et al., *Phys. Rev. B* **57**, 6689 (1998).
15. V. N. Popov and P. Lambin, *Phys. Rev. B* **73**, 085407 (2006).
16. N. Mounet and N. Marzari, *Phys. Rev. B* **71**, 205214 (2005).
17. C. Oshima, T. Aizava, R. Souda et al., *Sol. St. Comm.* **65**, 1601 (1988).
18. H. Yanagisawa, T. Tanaka, Y. Ishida et al., *Surf. Interface Anal.* **37**, 133 (2005).
19. *Graphite and Precursors*, ed. by P. Delhaes, Gordon and Breach, Australia (2001), Ch. 6.